

1 THE COMPARISON OF THREE REAL-TIME PCR KITS FOR SARS-COV-2 DIAGNOSIS
2 REVEALS DISCREPANCIES ON THE IDENTIFICATION OF POSITIVE COVID-19 CASES
3 AND DISPERSION ON THE VALUES OBTAINED FOR THE DETECTION OF SARS-COV-2
4 VARIANTS
5

6 Álvaro Santibáñez^{1,6}¶, Roberto Luraschi¹¶, Carlos Barrera-Avalos¹¶, Eva Vallejos-Vidal^{1,2}, Javiera
7 Alarcón¹, Javiera Cayunao¹, Andrea Mella¹, Maximiliano Figueroa¹, Felipe Hernández¹, Bárbara
8 Plaza¹, Ailen Inostroza-Molina¹, Daniel Valdés^{1,3}, Mónica Imarai^{1,3}, Claudio Acuña-Castillo^{1,3},
9 Felipe E. Reyes-López^{1,4,5,*}, Ana María Sandino^{1,3,*}.

10 ¹ Centro de Biotecnología Acuícola, Facultad de Química y Biología, Universidad de Santiago de
11 Chile, Santiago, Chile.

12 ² Centro de Nanociencia y Nanotecnología CEDENNA, Universidad de Santiago de Chile.

13 ³ Department of Biology, Faculty of Chemistry and Biology, University of Santiago de Chile,
14 Santiago, Chile.

15 ⁴ Department of Cell Biology, Physiology and Immunology, Universitat Autònoma de Barcelona,
16 Bellaterra, Spain.

17 ⁵ Facultad de Medicina Veterinaria y Agronomía, Universidad de Las Américas, Santiago, Chile.

18 ⁶ Programa Disciplinario de Inmunología, Instituto de Ciencias Biomédicas, Facultad de Medicina,
19 Universidad de Chile, Santiago, Chile.

20 ¶: These authors contributed equally to this work

21 * Corresponding author: Felipe.Reyes@uab.cat; felipe.reyes.1@usach.cl (Felipe E. Reyes-López)
22 ana.sandino@usach.cl (A.M. Sandino)

23 **ABSTRACT**

24 The COVID-19 pandemic has generated a huge challenge and threat to public health throughout the
25 world population. Reverse transcription associated with real-time Polymerase Chain Reaction (RT-
26 qPCR) has been the gold-standard molecular tool for diagnosis and detection of the SARS-CoV-2.
27 Currently, it is used as the main strategy for testing, traceability, and control of positive cases For
28 this reason, the on-top high demand for reagents has produced stock-out on several occasions and
29 the only alternative to keep population diagnosis has been the use of different RT-qPCR kits.
30 Therefore, we evaluate the performance of three of the commercial RT-qPCR kits currently in use
31 for SARS-CoV-2 diagnosis in Chile, consisting in: TaqMan 2019-nCoV Assay Kit v1 (Thermo).
32 Real-Time Fluorescent RT-PCR Kit for Detecting SARS-CoV-2 (BGI), and LightCycler®
33 Multiplex RNA Virus Master (Roche). Results of quantification cycle (Cq) and relative
34 fluorescence units (RFU) obtained from their RT-qPCR reactions revealed important discrepancies
35 on the total RNA required for the identification of SARS-CoV-2 genes and diagnosis. Marked
36 differences between kits in samples with 30>Cq value< 34 was observed. Samples with positive
37 diagnoses for Covid-19 using the Thermo Fisher kit had different results when the same samples
38 were evaluated with Roche and BGI kits. The displacement on the Cq value for SARS-CoV-2
39 identification between the three different RT-qPCR kits was also evident when the presence of
40 single nucleotide variants was evaluated in the context of genomic surveillance. Taken together, this
41 study emphasizes the special care adjusting RT-qPCR reaction conditions of the different kits must
42 be taken by all the laboratories before carrying out the detection of SARS-CoV-2 genes from total
43 RNA nasopharyngeal swab (NPS) samples.

44 Keywords: SARS-CoV-2 genomic surveillance; COVID-19 diagnosis; false-negative RT-qPCR
45 cases; SARS-CoV-2 variants detection; SARS-CoV-2 genomic surveillance.

46 1. INTRODUCTION

47 Coronavirus disease 2019 (COVID-19) is caused by the severe acute respiratory syndrome
48 coronavirus 2 (SARS-CoV-2). Since it was declared a pandemic by the World Health Organization
49 (WHO) on March 11, 2020 [1], it has generated a huge challenge and threat to public health
50 throughout the world population. This has forced governments to take a series of health measures to
51 control its spread, which mainly depend on the effective and timely diagnosis of infected people [2].
52 The Reverse transcription associated with real-time Polymerase Chain Reaction (RT-qPCR) has
53 been the gold-standard molecular tool for diagnosis and detection of the SARS-CoV-2 virus
54 recommended and, consequently, the most used strategy for testing, traceability, and isolation of
55 positive cases at present [3]. For this reason, it is not a surprise the use of supplies and kits for the
56 performance of this technique in diagnostic laboratories has increased [4]. To provide the supply
57 chain, a series of RT-qPCR kits for SARS-CoV-2 detection have been manufactured and are
58 currently available on market. Because the on-top high demand for reagents, in many opportunities
59 on which there have been situations of stock-out, the only alternative to maintain the diagnosis of
60 the population has been the use of alternative RT-qPCR kits. Thus, it is essential to analyze,
61 compare and clinically validate the performance of these commercial detection kits, to guide an
62 accurate diagnosis for this and other emerging infectious diseases.

63 The diagnosis of COVID-19 has been based on the detection of a series of target viral genes used
64 most frequently for the detection of SARS-CoV-2 by means of the RT-qPCR technique. For
65 example, the detection includes viral RNA of structural proteins such as envelope (E), nucleocapsid
66 (N) and spike (S) and a large open reading frame 1ab (ORF1ab), which encode non-structural
67 proteins, such as RNA-dependent RNA polymerase (RdRp) [5]. Along these lines, Van Kasteren P,
68 et al 2020, demonstrated and compared the performance of a series of commercially available RT-
69 qPCR Kits, which detect, for example, RdRp and S protein (KH Medical Kit) or ORF1ab and N
70 protein (CerTest Biotec Kit) with $\geq 96\%$ detection efficiency [6]. On the other hand, Kyu-Hwa H et
71 al, 2020, reported a comparison of commercial RT-qPCR Kits approved by emergency use in
72 Korea, which mainly detected E, N and RdRp proteins, with different detection specificity[7].
73 However, despite the publications on the RT-qPCR Kit analysis found in the market for the
74 diagnosis of COVID19, it is still essential to clinically validate those that have not been considered
75 to date, even in their performance in the detection of viral variants such as B.1.1.7 (Alpha), B.1.351
76 (Beta) and P.1 (Gamma) variants.

77 In this work we evaluate the performance of three commercial RT-qPCR kits for SARS-CoV-2
78 diagnosis, including TaqMan 2019-nCoV Assay Kit v1 (Thermo Fisher), the Real-Time Fluorescent
79 RT-PCR Kit for Detecting SARS-CoV-2 (BGI), and the LightCycler® Multiplex RNA Virus
80 Master (Roche). We report differences in the Cq values and RFU between kits on both, the
81 reference control and SARS-CoV-2 target genes. We also assessed the impact of the COVID-19
82 diagnosis upon the detection of SARS-CoV-2 single nucleotide variants. Our results highlight the
83 relevance to adjust RT-qPCR reaction conditions of the different kits by all the laboratories before
84 carrying out the detection of SARS-CoV-2 genes from total RNA extracted from NPS samples.

85 2. MATERIALS AND METHODS

86 **2.1 Samples.** Nasopharyngeal swab samples (NPSs) of clinical patients included in this study, were
87 collected by the Primary Care Centers and the Hospitals that belongs to the Central Metropolitan
88 Health Service (Santiago of Chile) (SSMC by its acronym in Spanish). The swab samples were
89 taken, preserved and transported using the Genosur sampling and transport kit (catalog number:
90 DM0001VR; Genosur LLC, NW) that contains an RNA stabilization buffer called DNA/RNA
91 Shield (Zymo Research Corp. Irvine, CA) that immediately provoke virus inactivation potentially
92 present in the sample. All the samples arrived at the laboratory before the first 24 hours after the
93 sampling collection. These samples were processed in the laboratory of Virology (University of

94 Santiago of Chile, USACH) in our role of laboratory of SARS-CoV-2 diagnostics that was member
95 of the University laboratories network developed in Chile for increasing the diagnostic capacity at
96 national level.

97 **2.2 Total RNA extraction.** Total RNA extraction was carried out using the Total RNA purification
98 kit (96 deep well plate format; Norgen Biotek Corp; Canada). Briefly, 250 μ L of NPS from each
99 patient was collected in a 1.5 ml tube and vortexed with 500 μ L of lysis buffer (buffer RL: absolute
100 ethanol; 1:1) during 1 min. Then, the solution was centrifuged at 14,000 x g for 5 min at room
101 temperature. Subsequently, 700 μ L of the lysate was transferred to a 96-filter plate and centrifuged
102 at 1690 x g for 6 min. The 96-filter plate was washed twice with 400 μ L of wash solution A. After
103 each wash the plate was centrifuged at 1690 x g for 4 min. Then, the plate was centrifuged at 1690 x
104 g for 10 min to any volume trace. Finally, the total RNA was eluted using 70 μ L of Elution solution
105 A and centrifuged at 1690 x g for 7 min. The purified RNA was evaluated immediately by RT-PCR.

106 **2.3 SARS-CoV-2 detection by RT-qPCR.** Three different kits for the SARS-CoV-2 detection
107 were evaluated. The detection of viral SARS-COV-2 genome sequence was carried out using the
108 ORF1ab probe (TaqMan™ 2019nCoV Assay Kit v1 (Thermo Fisher Scientific, Cat. No. A47532))
109 using a one-step strategy. Positive internal control probes for ORF1ab and RNase P (TaqMan™
110 2019-nCoV Control Kit v1; Thermo Fisher Scientific, Cat. No. A47533) were included and
111 assessed individually in the 96-well PCR plate. The polymerase from TaqMan™ Fast Virus 1-Step
112 Master Mix (Applied Biosystems™, Cat. No. 44-444-36) was included in each reaction. Each
113 reaction contained 5 μ l of TaqMan™ Fast Virus 1-Step Master Mix 4X, 1 μ l of ORF1ab assay 20X
114 (FAM detector channel), 1 μ l of RNase P assay 20X (HEX detector channel), 11 μ l of nuclease-free
115 water, and 2 μ l of extracted RNA sample. When 5 μ l of extracted RNA was used as template, 8 μ l
116 of nuclease-free water were dispensed in the reaction. The amplification thermal conditions include
117 the reverse transcription at 50 °C for 5 minutes, predenaturation at 95 °C for 20 s, followed by 45
118 cycles at 95 °C for 3 seconds and 60 °C for 30 seconds. The BGI kit detects viral SARS-COV-2
119 genome sequence using the ORF1ab probe (Real-Time Fluorescent RT-PCR Kit for Detecting
120 SARS-CoV-2 (BGI Health (HK) Co. Ltd, China, Cat. No. MFG030010)) using a one-step strategy.
121 Positive internal control probes for ORF1ab and β -actin were included and assessed individually in
122 the 96-well PCR plate. The polymerase from BGI Reaction Mix (BGI Health (HK) Co. Ltd, China,
123 Cat. No. MFG030010) was included in each reaction. Each reaction contained 18.5 μ l of SARS-
124 CoV-2 Reaction Mix (HEX detector channel to β -actin and FAM detector channel to ORF1ab), 1.5
125 μ l SARS-CoV-2 Enzyme Mix, 8 μ l of nuclease-free water, and 2 μ l of extracted RNA sample.
126 When 10 μ l of extracted RNA was used as template, nuclease-free water was not dispensed in the
127 reaction. The amplification thermal conditions include the reverse transcription at 50 °C for 5
128 minutes, predenaturation at 95 °C for 20 s, followed by 45 cycles at 95 °C for 3 seconds and 60 °C
129 for 30 seconds. The LightCycler® Multiplex RNA Virus Master kit detects viral SARS-COV-2
130 genome sequence using the RdRP probe (LightMix® Modular Wuhan CoV RdRP-gene. Cat. No.
131 53-0777-96) using a one-step strategy. Positive internal control probe for RdRP (LightMix®
132 Modular Wuhan CoV RdRP-gene. Cat. No. 53-0777-96) was included and assessed individually in
133 the 96-well PCR plate. As reference control, the RNase P probe (TaqMan™ 2019-nCoV Control
134 Kit v1; Thermo Fisher Scientific, Cat. No. A47533) was included for ensuring the presence of total
135 RNA extracted from NPS samples as template. This decision was supported on the antecedent the
136 Roche RT-qPCR kit utilized the Equine Arteritis Virus (EAV) as an internal control for the
137 extraction process but not a control of the total RNA extracted. The polymerase from RT-qPCR
138 Reaction Mix 5x (The LightCycler® Multiplex RNA Virus Master kit, Cat. No. 06754155001) was
139 included in each reaction. Each reaction contained 0.5 μ l of RdRP (FAM detector channel), 4 μ l of
140 RT-qPCR Reaction Mix 5x, 0.1 μ L of RT Enzyme Solution 200x, 1 μ L of RNase P probe, 12.4 μ l
141 of nuclease-free water, and 2 μ l of extracted RNA sample. When 5 μ l of extracted RNA was used
142 as template, 9.4 μ l of nuclease-free water were dispensed in the reaction. The amplification thermal
143 conditions include the reverse transcription at 50 °C for 10 minutes, predenaturation at 95 °C for 30

144 s, followed by 45 cycles at 95 °C for 5 seconds and 60 °C for 30 seconds. All the RT-qPCR
145 reactions were performed on the Agilent AriaMx Real-Time PCR System (Agilent Technologies,
146 Part. No. G8830A). Data and graphics were extracted using the Agilent AriaMx software.

147

148 **2.4 PCR efficiency and detection limit**

149 To establish PCR efficiency and the detection limit for both the reference (RNase P for Thermo
150 Fisher and Roche RT-qPCR kits; beta-actin for BGI kit) and the viral genes assessed (ORF1ab for
151 Thermo Fisher and BGI kits; RdRP for Roche kit) we ran RT-qPCR reactions using serial dilutions.
152 In order to get the maximum representation of values in the curve, we used for the 10-fold serial
153 dilutions a reference pool made from randomized ten total RNA NPS-extracted samples with a Cq
154 value around 20. The reactions were carried out in triplicate according to the specific conditions
155 indicated by the manufacturer and described above. All the RT-qPCR reactions were performed on
156 the Agilent AriaMx Real-Time PCR System. We determined the slope by linear regression in
157 GraphPad Prism and defined the required levels for PCR efficiency (E) and R-squared (R^2) as >95
158 % and >0.95, respectively. The primer efficiency was calculated according to the formula Efficiency
159 % (E) = $(10^{(-1/\text{Slope})-1}) \times 100$ [8]. To determine an approach about the detection limit we select ten
160 samples with Cq values above 30. To determine the minimum detection limit for each RT-qPCR
161 SARS-CoV-2 detection kit, a standard curve for the amplification of each probe assessed was
162 generated. The detection limit was established based on the last dilution on all the triplicates
163 amplified. We also took into consideration the R^2 (intended as a goodness-of-fit measure for linear
164 regression) and the probe efficiency (closer to 100%, intended 100% as the optimum probe
165 efficiency value).

166 **2.5 SARS-CoV-2 variants detection.** The detection of different variants was made by the
167 AccuPower® SARS-CoV-2 Variants ID Real-Time RT-PCR kit (Bioneer Cat. No. SMVR-2112)
168 according to manufacturer conditions as described elsewhere [9]. The Exicycler 96 V4 Real Time
169 thermal cycler (Bioneer) was used for detecting fluorescence on the TET, TexasRed, FAM,
170 TAMRA and Cyanine5 channels. Briefly, the reaction mix was prepared using 5 µL of Oligo Mix 1
171 (ID 1, which detects conventional SARS-CoV-2, the Hv69 / 70 DEL and N501Y mutation) or 5 µL
172 of Oligo Mix 2 (ID2, which detects the P681H mutation, E484K and K417N/T), 5 µL of Enzyme
173 Mix and 8 µL of nuclease-free water. Subsequently, to the 18 µL of Reaction Mix containing Oligo
174 Mix 1 or Oligo Mix 2, 2 µL of RNA extracted from samples routinely collected from COVID-19
175 positive patients were added. The thermal profile consists of a reverse transcription phase for 15
176 minutes at 50 °C and an activation phase at 95 °C for 5 minutes. Then, for PCR reaction 45
177 amplification cycles were run with a denaturation phase for 5 seconds at 95°C, an annealing /
178 extension phase for 30 seconds at 57°C and a scan phase within each cycle for the different probes.
179 The data obtained was exported in an Excel spreadsheet and the Cq value and fluorescence relative
180 intensity was analyzed for the internal positive control, IPC (TAMRA) and each one of the variants
181 assessed.

182 **2.6 Ethics statement.** All the experimental procedures included in this study was authorized by the
183 Ethical Committee of the University of Santiago of Chile (No. 226/2021) and the Scientific Ethical
184 Committee of the Central Metropolitan Health Service, Ministry of Health, Government of Chile
185 (No. 370/2021), and following the Chilean law in force. Patients interested in knowing their
186 diagnosis of the presence of SARS-CoV-2 were notified verbally in the same Family Health Center
187 (CESFAM, for its acronym in Spanish; Central Metropolitan Health Service, Ministry of Health ,
188 Government of Chile) to which they attended on their own. Verbal consent was detailed by the
189 health professional assigned by CESFAM for this purpose. Once their consent was given, the
190 patient gave their data to the health professional to identify, trace, and isolate a possible positive
191 case of Covid-19. Once the sample was received in the diagnostic laboratory, the person in charge
192 of the sample reception team (Dr. Claudio Acuña-Castillo) assigned an internal sample code to

193 ensure the traceability of the sample. Thus, data analysis used for this study was conducted only
194 using the internal sample code numbers assigned at the moment to receive the nasopharyngeal swab
195 samples for diagnostics purpose. Accordingly, the samples have been irreversible anonymized for
196 analysis and interpretation of results by the diagnostic laboratory team. Once assigned the
197 diagnostic result for each sample, Dr. Acuña-Castillo was responsible for communicating the result
198 to the CESFAM of origin for each sample.

199 **2.7 Data representation and statistical analysis.** A paired two-sided Student T-test was used to
200 determine differences between the Cq and RFU obtained from the different SARS-CoV-2 RT-qPCR
201 detection kits. A p -value of $p < 0.05$ was considered statistically significant. GraphPad Prism 8
202 statistical software was used to analyze and plot the data obtained.

203

204 3. RESULTS

205 The analysis of the extracted NPS samples with the Thermo Fisher RT-qPCR kit using 5 μ l
206 (according to the manufacturer instructions) and 2 μ l of total RNA revealed important differences
207 both in the quantification cycle (Cq) and in the relative fluorescence units (RFU) determined by the
208 RNase P (reference gene) and ORF1ab (SARS-CoV-2 gene) amplification (Fig 1). From a global
209 perspective, the 2 μ l of total RNA template decreased the Cq value in most of the samples assessed
210 compared to the 5 μ l of total RNA template (Fig 1A). This first perception is reinforced when the
211 mean \pm SD is represented, showing a lower Cq mean value for the 2 μ l of total RNA template
212 (14.09 ± 0.99) than the 5 μ l of total RNA template (14.82 ± 0.98) (Fig 1B). The same behavior was
213 also observed for the RFU, registering a strong difference between both volume of templates (Fig
214 1C) and determined by a higher mean fluorescence for the 2 μ l of total RNA template ($8969 \pm$
215 1232) than the 5 μ l of total RNA template (4041 ± 981) (Fig 1D). When the presence of SARS-
216 CoV-2 genome was evaluated by RT-qPCR in the total RNA extracted from NPS samples, those
217 three samples diagnosed as COVID-19 positive using 5 μ l of total RNA showed quite similar Cq
218 values using 2 μ l of total RNA as template (from lower to higher Cq value: Cq_{5 μ l}= 21.96 and
219 Cq_{2 μ l}=21.10; Cq_{5 μ l}= 35.13 and Cq_{2 μ l}= 36.69; Cq_{5 μ l}= 36.15 and Cq_{2 μ l}= 36.53) (Fig 1E). However,
220 other three total RNA NPS-extracted samples diagnosed as COVID-19 negative using the 5 μ l of
221 total RNA was diagnosed as COVID-19 positive with a template of 2 μ l of total RNA (Cq_{5 μ l}= 46.00
222 and Cq_{2 μ l}= 35.18; Cq_{5 μ l}= 46.00 and Cq_{2 μ l}= 36.92; Cq_{5 μ l}= 39.99 and Cq_{2 μ l}= 37.03). Based on these
223 results, it is not a surprise that the Cq mean for the 2 μ l of total RNA template (36.39 ± 5.02) was
224 lower than the 5 μ l of total RNA template (40.44 ± 7.29) (Fig 1F). In the same way than it was
225 observed for the amplification of the RNase P reference gene, all the total RNA NPS-extracted
226 samples registered a much higher fluorescence for the 2 μ l compared to the 5 μ l of total RNA as
227 template (Fig 1G). Thus, the 2 μ l of total RNA triplicated its mean fluorescence value ($1705 \pm$
228 1553) in comparison with the 5 μ l of total RNA (544.6 ± 562.3) (Fig 1H). The results with Thermo
229 Fisher RT-qPCR kit suggest a higher sensitivity of SARS-CoV-2 using 2 μ l of total RNA instead
230 the 5 μ l recommended by the manufacturer.

231

232 The BGI RT-qPCR kit registered also differences between the volume recommended by the
233 manufacturer (10 μ l) and 2 μ l of total RNA. At first sight, the amplification of beta-actin (internal
234 control) showed apparently a slight lower Cq values for the 10 μ l of total RNA template in most of
235 the samples assessed compared to the 2 μ l of total RNA template (Fig 2A). This data is supported
236 by the mean \pm SD of all analyzed samples, effectively showing a slight decrease on the Cq mean
237 value for the 10 μ l of total RNA template (23.21 ± 1.25) than the 2 μ l of total RNA template (23.58
238 ± 1.20) (Fig 2B). By contrast, the opposite trend observed for Cq values was observed for RFU,
239 noting an apparent higher fluorescence when it was used a volume of 2 μ l of total RNA as template

240 (Fig 2C). This perception is confirmed by the higher RFU mean using 2 μ l (4216 ± 698.5) than the
241 10 μ l of total RNA template (3724 ± 860.5) (Fig 2D). When the presence of SARS-CoV-2 was
242 evaluated in the total RNA NPS-extracted samples, very similar results were observed between the
243 paired Cq values for 10 and 2 μ l of total RNA (Fig 2E). However, four samples diagnosed as
244 COVID-19 negative with 10 μ l of total RNA were determined as COVID-19 positive when 2 μ l of
245 total RNA were dispensed ($Cq_{10\mu l} = 39.66$ and $Cq_{2\mu l} = 31.77$; $Cq_{10\mu l} = 46.00$ and $Cq_{2\mu l} = 35.05$; $Cq_{10\mu l} =$
246 46.00 and $Cq_{2\mu l} = 33.54$; $Cq_{10\mu l} = 46.00$ and $Cq_{2\mu l} = 28.79$) (Fig 2F). This result is influencing upon a
247 slight lower Cq mean value for SARS-CoV-2 ORF1ab detection with 2 μ l (27.70 ± 7.16) than 10 μ l
248 (29.64 ± 9.52). In the same way than it was observed for the amplification of the Beta-actin
249 reference gene, all the total RNA NPS-extracted samples registered a much higher fluorescence for
250 the 2 μ l (4093 ± 1568) compared to the 10 μ l of total RNA as template (2685 ± 1816) (Fig 2G-H).
251 These results with the BGI RT-qPCR kit suggest a higher sensitivity of SARS-CoV-2 using 2 μ l of
252 total RNA instead the 10 μ l recommended by the manufacturer.

253

254 The Roche RT-qPCR kit registered some differences between the volume recommended by the
255 manufacturer (5 μ l) and 2 μ l of total RNA, being most of them identified in the SARS-CoV-2 RdRP
256 gene. Looking at the paired Cq values for the RNase P reference gene, the 2 μ l of total RNA
257 template showed quite similar Cq values for most of the samples assessed compared to the 5 μ l of
258 total RNA template (Fig 3A). In fact, although the RNase P Cq mean value for 2 μ l was slightly
259 lower (18.22 ± 1.76) than 5 μ l of template (18.63 ± 1.92), no significant differences were observed
260 between them (Fig 3B). The same trend was also observed for the RFU, registering a marked
261 difference between both volume of templates (Fig 3C) and determined by a higher mean
262 fluorescence for the 2 μ l of total RNA template (6351 ± 812) than the 5 μ l of total RNA template
263 (4928 ± 849) (Fig 3D). The SARS-CoV-2 RdRP gene amplification showed quite similar paired Cq
264 values in most of the cases evaluated. In fact, seventeen of the twenty-five samples were diagnosed
265 as COVID-19 positive using both 5 μ l and 2 μ l of total RNA (Fig 3E). However, other two total
266 RNA NPS-extracted samples diagnosed as COVID-19 negative using the 5 μ l of total RNA was
267 diagnosed as COVID-19 positive using 2 μ l of total RNA as template ($Cq_{5\mu l} = 46.00$ and $Cq_{2\mu l} =$
268 35.53 ; $Cq_{5\mu l} = 40.33$ and $Cq_{2\mu l} = 31.85$) (Fig 3E). This difference in the diagnosis for those two
269 samples is probably the main responsible of the slight lower RdPR Cq-value differences registered
270 for the 2 μ l of total RNA template (30.62 ± 6.64) than the 5 μ l of total RNA template (33.02 ± 9.14)
271 (Fig 3F). Similarly to the amplification observed for the RNase P reference gene, it was also
272 observed a higher fluorescence on the amplification for RdRP with 2 μ l compared to the 5 μ l of
273 total RNA as template (Fig 3G). Thus, the mean fluorescence for the 2 μ l of total RNA was greater
274 (1738 ± 478) than 5 μ l of total RNA (1155 ± 580) (Fig 3H). The results with Roche RT-qPCR kit
275 confirm the higher sensitivity of SARS-CoV-2 using 2 μ l of total RNA instead the volume
276 recommended by the manufacturer.

277

278 To evaluate the performance of the three RT-qPCR, we compared the Cq, RFU and COVID-19
279 diagnosis on 90 randomized total RNA NPS-extracted samples. The amplification of the reference
280 gene showed clear differences between the RT-qPCR kits assessed, showing a greater Cq value on
281 most of the samples evaluated with the Thermo Fisher kit (Fig 4A). By contrast, the samples
282 amplified with the BGI kit showed the lower Cq value, even identifying two samples behind the
283 beta-actin detection limit (Fig 4A). The differences observed for the RNase P paired data was
284 confirmed with the Cq mean value for each kit, noting the highest Cq mean value for the Thermo
285 Fisher kit (16.55 ± 2.37), followed by the Roche kit (18.28 ± 2.03), and the BGI kit (28.01 ± 3.01)
286 (Fig 4B). The same profile was observed for the reference gene paired data amplification (Fig 4C),
287 noting the greatest and the lowest Cq mean values for the Thermo Fisher (7351 ± 1109) and the

288 BGI kits (2416 ± 482), respectively (Fig 4D). Importantly, the amplification profile observed for the
289 reference gene was not the same for the SARS-CoV-2 gene amplification. The paired Cq data
290 showed the greater Cq value for the Thermo Fisher kit but now followed by the BGI instead the
291 Roche kit, although no significant differences were observed between the BGI and the Roche kit
292 because the similar Cq mean value for both kits (29.63 ± 6.87 ; 29.94 ± 6.08) (Fig 4E). Importantly,
293 the differences between the Cq mean value on the viral gene for Thermo Fisher kit (27.24 ± 5.65)
294 and the other two kits is probably the responsible of the discrepancies observed in the COVID-19
295 positive diagnosis for the samples evaluated (23 positive samples diagnosed by Thermo Fisher; 18
296 positive samples diagnosed by BGI; 17 positive samples diagnosed by Roche) (Fig 4I). At fluoresce
297 level, the paired and mean values showed the same trend than the Cq values, although highlighting
298 the statistical difference also observed between the BGI and Roche RT-qPCR kits (Fig4 G-H).

299 Based on these results, we hypothesize that the discrepancies observed between the RT-qPCR kits
300 evaluated were focused on total RNA NPS-extracted with a high Cq (Cq > 30). Thus, the
301 comparison for the SARS-CoV-2 diagnostic performance was evaluated between the Thermo
302 Fisher, BGI and Roche RT-qPCR kits using ten randomized NPS samples with low Cq value ($19 <$
303 $Cq \text{ value} < 25$ for the ORF1ab amplification using the Thermo Fisher RT-qPCR kit), and other ten
304 randomized NPS samples with high Cq value ($30 < Cq \text{ value} < 34$ for the ORF1ab amplification
305 using the Thermo Fisher RT-qPCR kit). The reference gene amplification showed differences for
306 the paired Cq values between the RT-qPCR kits both for those samples identified with low Cq value
307 and high Cq value (Fig 5A; Fig 5I). Both in the low and high Cq value sample cases, the reference
308 gene amplification was greater for the Thermo Fisher kit (21.56 ± 1.40 ; 23.84 ± 1.04), followed by
309 the Roche kit (22.86 ± 1.54 ; 24.75 ± 1.15), and the BGI kit (28.54 ± 1.03 ; 29.86 ± 1.66) (Fig 5B;
310 Fig 5J). The differences for the paired RFU between kits had the same trend than it was observed
311 for Cq values, although even more marked when the RT-qPCR kit were compared (Fig 5C; Fig 5K).
312 Thus, in those samples with low and high Cq values, the RFU was much greater in the case of
313 Thermo Fisher kit (7455 ± 734 ; 7431 ± 535), followed by the Roche kit (4381 ± 633 ; 5093 ± 695),
314 and the BGI kit (2154 ± 522 ; 1919 ± 228) (Fig 5D; Fig 5L). Importantly, when the amplification of
315 the viral gene was evaluated, it was not observed the same trend registered for the reference gene
316 amplification. In fact, in the paired-comparison perspective all the RNA NPS-extracted samples
317 with low and high Cq values showed the greater Cq viral gene amplification for the Thermo Fisher
318 kit but now followed by the BGI and the Roche kit (Fig 5E; Fig 5M). In this way, in the samples
319 with low Cq values, their mean values showed slight but significant differences between kits (22.03
320 ± 1.67 for Thermo Fisher; 23.69 ± 2.65 for BGI; 25.39 ± 3.66 for Roche) (Fig 5F). However, in the
321 case of the samples with high Cq values more marked differences between kits were registered
322 (31.98 ± 1.03 for Thermo Fisher; 34.27 ± 1.91 for BGI; 43.27 ± 3.66 for Roche) (Fig 5N). These
323 differences are probably attributable not only to the sensitivity of each kit but also to the number of
324 samples diagnosed as COVID-19 positive. Moreover, meanwhile in the case of samples with low
325 Cq value all the ten samples were reported with COVID-19 diagnosis (Fig 5Q), in the samples with
326 high Cq just all the ten samples were effectively confirmed with COVID-19 positive diagnosis by
327 Thermo Fisher but only seven and even no one sample were diagnosed using the BGI and Roche
328 kits, respectively (Fig 5N; Fig 5R). The same behavior trend in the RFU was observed for the low
329 and high Cq value samples, both in the paired (Fig 5G; Fig 5O) and RFU mean value obtained (Fig
330 5H; Fig 5P), respectively. These results indicate that the samples with Cq values greater than 30
331 could compromise its COVID-19 diagnosis depending on the kit used for this purpose.

332

333 To determine the distribution of positive samples and its impact on the detection of single
334 nucleotide polymorphisms (also called single nucleotide variants, SNV) associated to SARS-CoV-2
335 variants, we evaluated twelve total RNA samples with a Cq value lower than 26. As it was
336 expected, all the twelve samples were identified as SARS-CoV-2 positive samples. However, from

337 the twelve samples only six of them were also positive for the variants N501Y, K417N/T, and
338 E484K, suggesting the presence of the P1 (Gamma) SARS-CoV-2 variant in the 50% of the
339 samples (Fig 6A). By contrast, none of the samples were positive for Hv 69/70 del, and/or P681H.
340 According to our previous evidence, the Cq mean \pm standard deviation (mean \pm SD) for these
341 samples also showed a clear dispersion on the Cq distribution (Fig 6B). In fact, one of the samples
342 identified with the SARS-CoV-2 N501Y, K417N/T, and E484K SNV registered a Cq_{RdRP} value=
343 29.98 with the Roche RT-qPCR diagnostic kit (Fig 6B). The same sample showed a Cq_{ORF1ab} value=
344 25.71 and Cq_{ORF1ab} value= 27.13 for Thermo Fisher and BGI, respectively (Supplementary Fig 2).
345 This evidence suggests that the recommendation for using only samples with Cq < 30 made by the
346 manufacturer should have also in consideration the diagnostic RT-qPCR used for such purpose.

347

348 4. DISCUSSION

349 Prior work has documented comparisons between the efficacy of different commercial PCR
350 kits for the diagnosis of SARS-CoV-2 by RT-qPCR [6,10–12]. Lu et al 2020 [13], for example,
351 compared and analyzed the performance of Sansure and BioGerm, widely used in Liuzhou People's
352 Hospital in Guangxi, China, with an effectiveness of 80 and 94% respectively. On the other hand,
353 Eberle et al 2021 [13], compared nine RT-qPCR kits used in viral diagnosis in the city of Bavaria,
354 Germany. Mostly of them reached percentages of sensitivity between 90-100%, while others two
355 kits reported 49% (Fast Track Diagnostics Kit) or 62% (Wells Bio, Inc) of effectiveness with the
356 highest number of false negatives. However, the choice of Kits that have more than one target gene
357 been less susceptible to obtaining false negatives than tests designed to detect a single genetic
358 target, even in the detection of viral variants [14–16]. These studies suggest considering and
359 analyzing the performance of commercial RT-qPCR kits used locally in the analysis of COVID 19.
360 In fact, a poor performance in the diagnosis of SARS-COV-2 can favor the spread of this and other
361 infectious diseases in the future. In Chile, being the country with the most PCR tests performed per
362 million inhabitants in Latin America [17], no standardization, comparative or efficacy studies of
363 commercial RT-qPCR kits used in the mass diagnosis of local SARS-CoV-2, nor in the detection of
364 emerging variants, have been reported. We announces the first clinical validations and comparison
365 of the TaqMan 2019-nCoV Assay Kit v1 (Thermo Fisher), the Real-Time Fluorescent RT-PCR Kit
366 for Detecting SARS-CoV-2 (BGI) and the LightCycler® Multiplex RNA Virus Master (Roche)
367 commercial RT-qPCR Kits used to control the pandemic and diagnostic in the population of
368 Santiago, Chile. The Cq and the RFU obtained from their RT-qPCR reactions revealed important
369 discrepancies on the total RNA volume for the identification of SARS-CoV-2 genes and diagnosis.
370 Importantly, those differences had a marked impact on the identification of positive COVID-19
371 cases. Particularly in those samples with a 30 > Cq value < 34, from the ten samples with positive
372 diagnostic for COVID-19 using the Thermo Fisher kit, none of them had the same diagnostic when
373 were evaluated with the Roche kit. This evidence reinforces the need to standardize the total RNA
374 loading volume considering the specific conditions for each diagnostic laboratory. While the
375 Thermo Fisher Kit presents better general parameters in the diagnosis, even in the detection of
376 SNV. These findings are related to the evidence reported by Farfán et al, 2020 [18], work in which
377 the Thermo Fisher kit is indicated as a diagnostic gold standard. While some reports describe the
378 performance of in-house RNA SARS-CoV-2 extraction protocols, validating their results with the
379 same kit [19]. Others point out its compatibility to detect SARS-CoV-2 in nasopharyngeal samples
380 without prior RNA extraction [20], corroborating its good performance and sensitivity in viral
381 detection. On the other hand, while the BGI kit has shown a sensitivity of $\geq 95\%$ in other studies
382 [6], we obtained only 70.1%, possibly due to the random selection of positive samples without
383 considering high or low viral loads. Although in our study the Roche kit had lower RFU, high Cq
384 and less sensitivity compared to Thermo Fisher and BGI, studies indicate that Roche has sufficient
385 performance to detect positive cases and over other RT-qPCR kits, such as Cepheid [21] and Certest

386 Biotec SL. Our study reveals important differences between the Thermo Fisher, BGI and the Roche
387 RT-qPCR kit for SARS-CoV-2 diagnostic both in the Cq and the RFU values. In this way, we
388 consider that the fluorescence is also a parameter that should be carefully considered when
389 diagnosing a sample. The displacement on the Cq values for the SARS-CoV-2 genome
390 identification on total RNA NPS-extracted samples could not also affect their Covid-19 diagnosis
391 but also could, as consequence, compromise the identification of viral SNV in the context of
392 genomic surveillance. This study is the first that analyzes and compares the sensitivity and
393 performance of the RT-qPCR kits used in Chile and suggests an in-depth analysis of the new
394 commercial kits manufactured for the control of this and future infectious diseases.

395
396

397 5. REFERENCES

- 398 [1] Organization WH. Statement on the second meeting of the International Health Regulations.
399 Emergency Committee regarding the outbreak of novel coronavirus (2019-nCoV) 2021.
400 [https://www.who.int/news-room/detail/30-01-2020-statement-on-the-second-meeting-of-the-](https://www.who.int/news-room/detail/30-01-2020-statement-on-the-second-meeting-of-the-international-health-regulations-(2005)-emergency-committee-regarding-the-outbreak-of-novel-coronavirus-(2019-ncov))
401 [international-health-regulations-\(2005\)-emergency-committee-regarding-the-outbreak-of-](https://www.who.int/news-room/detail/30-01-2020-statement-on-the-second-meeting-of-the-international-health-regulations-(2005)-emergency-committee-regarding-the-outbreak-of-novel-coronavirus-(2019-ncov))
402 [novel-coronavirus-\(2019-ncov\)](https://www.who.int/news-room/detail/30-01-2020-statement-on-the-second-meeting-of-the-international-health-regulations-(2005)-emergency-committee-regarding-the-outbreak-of-novel-coronavirus-(2019-ncov)). (accessed July 8, 2021).
- 403 [2] Younes N, Al-Sadeq DW, Al-Jighefee H, Younes S, Al-Jamal O, Daas HI, et al. Challenges
404 in Laboratory Diagnosis of the Novel. *Viruses* 2020;12:582.
- 405 [3] Barreto HG, de Pádua Milagres FA, de Araújo GC, Daúde MM, Benedito VA. Diagnosing
406 the novel SARS-CoV-2 by quantitative RT-PCR: variations and opportunities. *J Mol Med*
407 2020;98:1727–36. <https://doi.org/10.1007/s00109-020-01992-x>.
- 408 [4] Kim S min, Hwang YJ, Kwak Y. Prolonged SARS-CoV-2 detection and reversed RT-PCR
409 results in mild or asymptomatic patients. *Infect Dis (Auckl)* 2021;53:31–7.
410 <https://doi.org/10.1080/23744235.2020.1820076>.
- 411 [5] Lv D, Ying Q, Weng Y, Shen C, Chu J. Dynamic change process of target genes by RT-
412 PCR testing of SARS-Cov-2 during the course of a Coronavirus Disease 2019 patient. *Clin*
413 *Chim Acta* 2020;506:172–5. <https://doi.org/10.1016/j.cca.2020.03.032>.
- 414 [6] van Kasteren PB, van der Veer B, van den Brink S, Wijsman L, de Jonge J, van den Brandt
415 A, et al. Comparison of seven commercial RT-PCR diagnostic kits for COVID-19. *J Clin*
416 *Virol* 2020;128:104412. <https://doi.org/10.1016/j.jcv.2020.104412>.
- 417 [7] Hur KH, Park K, Lim Y, Jeong YS, Sung H, Kim MN. Evaluation of Four Commercial Kits
418 for SARS-CoV-2 Real-Time Reverse-Transcription Polymerase Chain Reaction Approved
419 by Emergency-Use-Authorization in Korea. *Front Med* 2020;7:1–10.
420 <https://doi.org/10.3389/fmed.2020.00521>.
- 421 [8] Pfaffl MW. A new mathematical model for relative quantification in real-time RT-PCR.
422 *Nucleic Acids Res* 2001;29:e45. <https://doi.org/10.1093/nar/29.9.e45>.
- 423 [9] Young RM, Solis CJ, Barriga-fehrman A, Abogabir C, Álvaro R, Labarca M, et al.
424 Smartphone Screen Testing, a novel pre-diagnostic method to identify SARS-CoV-2
425 infectious individuals. *Elife* 2021:e70333. <https://doi.org/10.7554/elife.70333>.
- 426 [10] Iglói Z, Ieven M, Abdel-Karem Abou-Nouar Z, Weller B, Matheussen V, Coppens J, et al.
427 Comparison of commercial realtime reverse transcription PCR assays for the detection of
428 SARS-CoV-2. *J Clin Virol* 2020;129:4–6. <https://doi.org/10.1016/j.jcv.2020.104510>.
- 429 [11] Tastanova A, Stoffel CI, Dzung A, Cheng PF, Bellini E, Johansen P, et al. A Comparative

- 430 Study of Real-Time RT-PCR–Based SARS-CoV-2 Detection Methods and Its Application
431 to Human-Derived and Surface Swabbed Material. *J Mol Diagnostics* 2021;23:796–804.
432 <https://doi.org/10.1016/j.jmoldx.2021.04.009>.
- 433 [12] Zhao J, Zhang Y, Cao B. *Journal of Clinical Chemistry and Comparison of the Performance*
434 *of Six SARS-CoV-2 Nucleic Acid Detection Kit in Positive Samples Using RT-PCR*
435 2021;4:1–5.
- 436 [13] Lu Y, Li L, Ren S, Liu X, Zhang L, Li W, et al. Comparison of the diagnostic efficacy
437 between two PCR test kits for SARS-CoV-2 nucleic acid detection. *J Clin Lab Anal*
438 2020;34:1–5. <https://doi.org/10.1002/jcla.23554>.
- 439 [14] Eberle U, Wimmer C, Huber I, Neubauer-Juric A, Valenza G, Ackermann N, et al.
440 Comparison of nine different commercially available molecular assays for detection of
441 SARS-CoV-2 RNA. *Eur J Clin Microbiol Infect Dis* 2021;40:1303–8.
442 <https://doi.org/10.1007/s10096-021-04159-9>.
- 443 [15] U.S. Food and Drug Administration. Genetic Variants of SARS-CoV-2 May Lead to False
444 Negative Results with Molecular Tests for Detection of SARS-CoV-2 n.d.
445 [https://www.fda.gov/medical-devices/letters-health-care-providers/genetic-variants-sars-cov-](https://www.fda.gov/medical-devices/letters-health-care-providers/genetic-variants-sars-cov-2-may-lead-false-negative-results-molecular-tests-detection-sars-cov-2)
446 [2-may-lead-false-negative-results-molecular-tests-detection-sars-cov-2](https://www.fda.gov/medical-devices/letters-health-care-providers/genetic-variants-sars-cov-2-may-lead-false-negative-results-molecular-tests-detection-sars-cov-2) (accessed July 8,
447 2021).
- 448 [16] Kalita D, Deka S. Effectiveness of Different Gene-Target Strategies for SARS-CoV-2
449 Screening by RT-PCR and Other Modalities: A Scoping Review. *J Med Diagn Meth*
450 2020;9:298. <https://doi.org/10.35248/2168-9784.2020.9.298>.
- 451 [17] Burki T. Understanding variants of SARS-CoV-2. *Lancet* 2021;397:462.
452 [https://doi.org/http://dx.doi.org/10.1016/S0140-6736\(21\)00298-1](https://doi.org/http://dx.doi.org/10.1016/S0140-6736(21)00298-1).
- 453 [18] Statista. Rate of coronavirus (COVID-19) tests performed in the most impacted countries
454 worldwide. 2021-06-28 n.d. [https://www.statista.com/statistics/1104645/covid19-testing-](https://www.statista.com/statistics/1104645/covid19-testing-rate-select-countries-worldwide/)
455 [rate-select-countries-worldwide/](https://www.statista.com/statistics/1104645/covid19-testing-rate-select-countries-worldwide/) (accessed July 8, 2021).
- 456 [19] Farfan MJ, Torres JP, O’ryan M, Olivares M, Gallardo P, Lastra J, et al. Optimizing rt-pcr
457 detection of sars-cov-2 for developing countries using pool testing. *Rev Chil Infectol*
458 2020;37:276–80. <https://doi.org/10.4067/s0716-10182020000300276>.
- 459 [20] Lázaro-Perona F, Rodríguez-Antolín C, Alguacil-Guillén M, Gutiérrez-Arroyo A,
460 Mingorance J, García-Rodríguez J. Evaluation of two automated low-cost RNA extraction
461 protocols for SARS-CoV-2 detection. *PLoS One* 2021;16:1–10.
462 <https://doi.org/10.1371/journal.pone.0246302>.
- 463 [21] Cibali E, Wenzel JJ, Gruber R, Ambrosch A. Pooling for SARS-CoV-2-testing: Comparison
464 of three commercially available RT-qPCR kits in an experimental approach. *Clin Chem Lab*
465 *Med* 2021;59:E243–5. <https://doi.org/10.1515/cclm-2020-1375>.

466

467

468

469

470

471

472

473

474

475 FIGURES CAPTIONS

476

477 **Fig 1. Comparative analysis for the detection of SARS-CoV-2 from nasopharyngeal swab**
478 **(NPS) samples using RNase P and ORF1ab gene (Thermo Fisher RT-qPCR kit).** The
479 comparison was made from the same NPS sample using the recommended volume of extracted
480 RNA (5 μ l of total RNA, recommended by the manufacturer; red spots) and 2 μ l of total RNA (blue
481 spots). In the graphs, each spot is a different analyzed sample for each volume condition (5 μ l; 2
482 μ l). The line linking two spots indicated the paired result obtained for the same sample assessed
483 using the two different volume conditions. Samples with Cq= 46 denotes no amplification. (A)
484 Paired quantification cycle (Cq) analysis for the RNase P the amplification values obtained by RT-
485 qPCR for each sample assessed. (B) Cq mean \pm standard deviation (mean \pm SD) for the RNase P
486 amplification values obtained by RT-qPCR from all the samples evaluated. (C) Paired relative
487 fluorescence unit (RFU) analysis for the RNase P amplification values obtained by RT-qPCR for
488 each sample assessed. (D) RFU mean \pm standard deviation (mean \pm SD) amplification of RNase P
489 obtained by RT-qPCR from all the samples evaluated. (E) Paired Cq analysis for the SARS-CoV-2
490 ORF1ab gene amplification values obtained by RT-qPCR for each sample assessed. (F) Cq mean \pm
491 standard deviation (mean \pm SD) SARS-CoV-2 ORF1ab gene amplification obtained by Rt-qPCR
492 from all the samples evaluated. (G) Paired RFU analysis for the SARS-CoV-2 ORF1ab gene
493 amplification values obtained by Rt-qPCR for each sample assessed. (H) RFU mean \pm standard
494 deviation (mean \pm SD) of SARS-CoV-2 ORF1ab gene amplification obtained by RT-qPCR from all
495 the samples evaluated by RT-qPCR. For statistical analysis, paired two-sided Student T-test was
496 applied (n= 83 NPS samples chosen at random). * p<0.05; ** p<0.01; *** p<0.001; **** p<0.0001.

497

498 **Fig 2. Comparative analysis for the detection of SARS-CoV-2 from NPS samples using beta-**
499 **actin and ORF1ab gene (BGI RT-qPCR kit).** The comparison was made from the same NPS
500 sample using the recommended volume of extracted RNA (10 μ l of total RNA, recommended by
501 the manufacturer; red spots) and 2 μ l of total RNA (blue spots). In the graphs, each spot is a
502 different analyzed sample for each volume condition (10 μ l; 2 μ l). The line linking two spots
503 indicated the paired result obtained for the same sample assessed using the two different volume
504 conditions. Samples with Cq= 46 denotes no amplification. (A) Paired quantification cycle (Cq)
505 analysis for the beta-actin amplification values obtained by RT-qPCR for each sample assessed. (B)
506 Cq mean \pm standard deviation (mean \pm SD) for the beta-actin amplification values obtained by RT-
507 qPCR from all the samples evaluated. (C) Paired relative fluorescence unit (RFU) analysis for the
508 beta-actin amplification values obtained by RT-qPCR for each sample assessed. (D) RFU mean \pm
509 standard deviation (mean \pm SD) amplification of beta-actin obtained by RT-qPCR from all the
510 samples evaluated. (E) Paired Cq analysis for the SARS-CoV-2 ORF1ab gene amplification values
511 obtained by RT-qPCR for each sample assessed. (F) Cq mean \pm standard deviation (mean \pm SD)
512 SARS-CoV-2 ORF1ab gene amplification obtained by Rt-qPCR from all the samples evaluated. (G)
513 Paired RFU analysis for the SARS-CoV-2 ORF1ab gene amplification values obtained by RT-
514 qPCR for each sample assessed. (H) RFU mean \pm standard deviation (mean \pm SD) of SARS-CoV-2
515 ORF1ab gene amplification obtained by RT-qPCR from all the samples evaluated by RT-qPCR. For

516 statistical analysis, paired two-sided Student T-test was applied (n= 71 NPS samples chosen at
517 random). * p<0.05; ** p<0.01; *** p<0.001; **** p<0.0001.

518

519

520

521

522 **Fig 3. Comparative analysis for the detection of SARS-CoV-2 from NPS samples using RNase**
523 **P (as cellular reference gene) and RdRP gene (Roche RT-qPCR kit).** The comparison was made
524 from the same NPS sample using the recommended volume of extracted RNA (5 µl of total RNA,
525 recommended by the manufacturer; red spots) and 2 µl of total RNA (blue spots). In the graphs,
526 each spot is a different analyzed sample for each volume condition (5ul; 2 ul). The line linking two
527 spots indicated the paired result obtained for the same sample assessed using the two different
528 volume conditions. Samples with Cq= 46 denotes no amplification. (A) Paired quantification cycle
529 (Cq) analysis for the RNase P the amplification values obtained by RT-qPCR for each sample
530 assessed. (B) Cq mean ± standard deviation (mean ± SD) for the RNase P amplification values
531 obtained by RT-qPCR from all the samples evaluated. (C) Paired relative fluorescence unit (RFU)
532 analysis for the RNase P amplification values obtained by RT-qPCR for each sample assessed. (D)
533 RFU mean ± standard deviation (mean ± SD) amplification of RNase P obtained by RT-qPCR from
534 all the samples evaluated. (E) Paired Cq analysis for the SARS-CoV-2 RdRP gene amplification
535 values obtained by RT-qPCR for each sample assessed. (F) Cq mean ± standard deviation (mean ±
536 SD) SARS-CoV-2 RdRP gene amplification obtained by Rt-qPCR from all the samples evaluated.
537 (G) Paired RFU analysis for the SARS-CoV-2 RdRP gene amplification values obtained by RT-
538 qPCR for each sample assessed. (H) RFU mean ± standard deviation (mean ± SD) of SARS-CoV-2
539 RdRP gene amplification obtained by RT-qPCR from all the samples evaluated. For statistical
540 analysis, paired two-sided Student T-test was applied (n= 90 NPS samples chosen at random). *
541 p<0.05; ** p<0.01; *** p<0.001; **** p<0.0001.

542

543 **Fig 4 Comparative analysis for the detection of SARS-CoV-2 from NPS samples chosen at**
544 **random using the three RT-qPCR kits.** The comparison was made from the same NPS sample
545 using the optimized volume of total RNA extracted (2 µl). In the graphs, each spot for each RT-
546 qPCR kit is a different analyzed sample. The line linking the spots indicated the paired result
547 obtained for the same sample assessed by the different RT-qPCR kits. Samples with Cq= 46 denotes
548 no amplification. (A) Paired quantification cycle (Cq) analysis for the RNase P amplification values
549 obtained by RT-qPCR for each sample assessed. (B) Cq mean ± standard deviation (mean ± SD) for
550 the RNase P amplification obtained by RT-qPCR for all the samples evaluated. On (A) and (B), the
551 horizontal red (for Thermo Fisher), blue (for BGI), and green line (for Roche) indicates the
552 detection limit for the determination of the reference gene on each of the RT-qPCR kits (determined
553 on Supplementary Figure 1). (C) Paired relative fluorescence unit (RFU) analysis for the RNase P
554 amplification values obtained by RT-qPCR for each sample assessed. (D) RFU mean ± standard
555 deviation (mean ± SD) for the RNase P amplification obtained by RT-qPCR from all the samples
556 evaluated. (E) Paired Cq analysis for the SARS-CoV-2 ORF1ab gene amplification values obtained
557 by RT-qPCR for each sample assessed. (F) Cq mean ± standard deviation (mean ± SD) for the
558 SARS-CoV-2 gene amplification obtained by each one of the RT-qPCR assessed. On (E) and (F),
559 the horizontal red (for Thermo Fisher), blue (for BGI), and green line (for Roche) indicates the
560 detection limit for the determination of the viral gene on each of the RT-qPCR kits (determined on
561 Supplementary Figure 1). (G) Paired RFU analysis for the SARS-CoV-2 ORF1ab gene

562 amplification values obtained by RT-qPCR for each sample assessed. (H) RFU mean \pm standard
563 deviation (mean \pm SD) for the SARS-CoV-2 ORF1ab gene amplification obtained by RT-qPCR for
564 all the samples evaluated. (I) NPS samples with COVID-19 positive diagnostic obtained by each
565 one of the RT-qPCR kits assessed. For statistical analysis, paired two-sided Student T-test was
566 applied (n= 90 NPS samples chosen at random). * p<0.05; ** p<0.01; *** p<0.001; **** p<0.0001.

567

568

569 **Fig 5. Comparative analysis for the detection of SARS-CoV-2 from NPS samples with Cq< 25**
570 **as samples with low Cq value and 30<Cq<35 as samples with high Cq value using the three**
571 **RT-qPCR kits.** The comparison was made from the same NPS sample using the optimized volume
572 of total RNA extracted (2 μ l). In the graphs, each spot for each RT-qPCR kit is a different analyzed
573 sample. The line linking the spots indicated the paired result obtained for the same sample assessed
574 by the different RT-qPCR kits. Samples with Cq= 46 denotes no amplification. (A) Paired
575 quantification cycle (Cq) analysis for the RNase amplification values obtained by RT-qPCR from
576 samples evaluated with low Cq value. (B) Cq mean \pm standard deviation (mean \pm SD) for the
577 RNase P amplification obtained by RT-qPCR from samples evaluated with low Cq value. (C)
578 Paired relative fluorescence unit (RFU) analysis for the RNase P amplification values obtained by
579 RT-qPCR for each sample evaluated with low Cq value. (D) RFU mean \pm standard deviation (mean
580 \pm SD) for the RNase amplification obtained by RT-qPCR from samples evaluated with low Cq
581 value. (E) Paired Cq analysis for the SARS-CoV-2 gene amplification (ORF1ab for Thermo Fisher
582 and BGI; RdRP for Roche) obtained by RT-qPCR from the samples evaluated with low Cq value.
583 (F) Cq mean \pm standard deviation (mean \pm SD) for the viral gene amplification values obtained by
584 RT-qPCR from samples evaluated with low Cq value. (G) Paired relative fluorescence unit (RFU)
585 analysis for the viral gene amplification values obtained by RT-qPCR for each sample evaluated
586 with low Cq value. (H) RFU mean \pm standard deviation (mean \pm SD) for the viral gene
587 amplification obtained by RT-qPCR from samples evaluated with low Cq value. (I) Paired
588 quantification cycle (Cq) analysis for the RNase amplification values obtained by RT-qPCR from
589 samples evaluated with high Cq value. (J) Cq mean \pm standard deviation (mean \pm SD) for the
590 RNase P amplification obtained by RT-qPCR from samples evaluated with high Cq value. (K)
591 Paired relative fluorescence unit (RFU) analysis for the RNase P amplification values obtained by
592 RT-qPCR for each sample evaluated with high Cq value. (L) RFU mean \pm standard deviation (mean
593 \pm SD) for the RNase amplification obtained by RT-qPCR from samples evaluated with high Cq
594 value. (M) Paired Cq analysis for the SARS-CoV-2 gene amplification (ORF1ab for Thermo Fisher
595 and BGI; RdRP for Roche) obtained by RT-qPCR from the samples evaluated with high Cq value.
596 (N) Cq mean \pm standard deviation (mean \pm SD) for the viral gene amplification values obtained by
597 RT-qPCR from samples evaluated with high Cq value. On (M) and (N), the horizontal red (for
598 Thermo Fisher), blue (for BGI), and green line (for Roche) indicates the detection limit for the
599 determination of the viral gene on each of the RT-qPCR kits (determined on Supplementary Figure
600 1). (O) Paired relative fluorescence unit (RFU) analysis for the viral gene amplification values
601 obtained by RT-qPCR for each sample evaluated with high Cq value. (P) RFU mean \pm standard
602 deviation (mean \pm SD) for the viral gene amplification obtained by RT-qPCR from samples
603 evaluated with high Cq value. On (M) and (N), the horizontal red (for Thermo Fisher), blue (for
604 BGI), and green line (for Roche) indicates the detection limit for the determination of the viral gene
605 on each of the RT-qPCR kits. (Q) NPS samples with COVID-19 positive diagnostic obtained by the
606 RT-qPCR kits from samples with low Cq value. (R) NPS samples with COVID-19 positive
607 diagnostic obtained by the RT-qPCR kits from samples with high Cq value. For statistical analysis,
608 paired two-sided Student T-test was applied (n= 10 NPS samples with low Cq value; n= 10 NPS
609 samples with high Cq value). * p<0.05; ** p<0.01; *** p<0.001; **** p<0.0001.

610

611 **Fig 6. Screening and identification of SARS-CoV-2 single nucleotide variants following a RT-**
612 **qPCR strategy.** We included twelve total RNA samples extracted from nasopharyngeal swab
613 (NPS) specimens with $Cq < 30$ chosen at random. (A) Identification of SARS-CoV-2 positive
614 samples, and the SNV N501Y, K417N/T, E484K, Hv 69/70 del, and/or P681H. From the twelve
615 samples, only the single identification of SARS-CoV-2 was registered on six samples. The other six
616 samples were SARS-Cov-2 positive and also positive for the SNV N501Y, K417N/T, and E484K.
617 None of the samples were positive for SNV Hv 69/70 del, and/or P681H. (B) Cq mean \pm standard
618 deviation (mean \pm SD) for the SARS-CoV-2 gene amplification obtained by each one of the RT-
619 qPCR assessed (red: Thermo Fisher; blue: BGI; Green: Roche).

620

621 **Supplementary Fig 1. Standard amplification curves to determine the probe efficiency and**
622 **detection limit for the Thermo Fisher, BGI, and Roche RT-qPCR kits.** The left and right
623 column show the amplification for the reference and the SARS-CoV-2 gene, respectively. The
624 analysis included 10-fold serial dilutions from a reference pool made from randomized ten total
625 RNA NPS-extracted samples with a Cq value around 20. The reactions were carried out in triplicate
626 according to the specific conditions indicated by the manufacturer. (A) Amplification curve using
627 the RNase P probe (Thermo Fisher RT-qPCR kit). (B) Amplification curve using the SARS-CoV-2
628 ORF1ab probe (Thermo Fisher RT-qPCR kit). (C) Amplification curve using the beta-actin probe
629 (BGI RT-qPCR kit). (D) Amplification curve using the SARS-CoV-2 ORF1ab probe (BGI RT-
630 qPCR kit). (E) Amplification curve using the ORF1ab probe (Thermo Fisher RT-qPCR kit; reaction
631 mix prepared with the Roche RT-qPCR kit). (F) Amplification curve using the SARS-CoV-2 RdRP
632 probe (Roche RT-qPCR kit). All the graphs represent the linear equation ($y = a + bx$, $b =$ slope and
633 $a =$ y-intercept), R -squared (R^2), and the percentage probe efficiency (%Eff). The dotted line
634 indicates the Cq value at which the detection limit was set for each probe assessed for Thermo
635 Fisher ($Cq_{RNaseP}=.36.92$; $Cq_{ORF1ab}=.37.15$), BGI ($Cq_{beta-actin}=.38.44$; $Cq_{ORF1ab}=.35.07$), and Roche RT-
636 qPCR kit ($Cq_{RNaseP}=.38.11$; $Cq_{ORF1ab}=.35.65$).

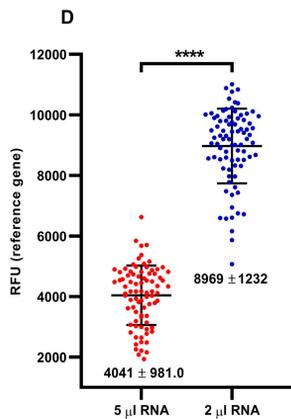
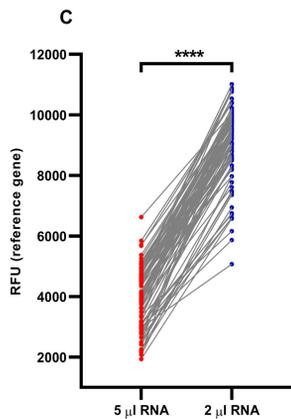
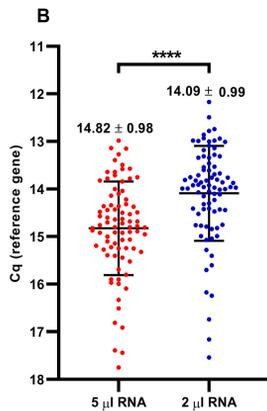
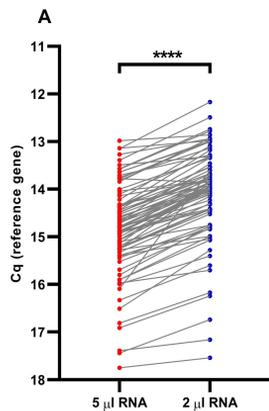
637

638 **Supplementary Fig 2. Amplification performance for the samples included in the detection of**
639 **SARS-CoV-2 single nucleotide variants (SNV).** Total RNA extracted from nasopharyngeal swab
640 (NPS) samples ($n = 12$) with $Cq < 30$ chosen at random were screened using three different RT-
641 qPCR kits (Thermo Fisher (red); BGI (blue); Roche (green)). The comparison was made from the
642 same NPS sample using the optimized volume of total RNA extracted ($2 \mu l$). In the graphs, each
643 spot for each RT-qPCR kit is a different analyzed sample. The line linking the spots indicated the
644 paired result obtained for the same sample assessed by the different RT-qPCR kits. (A) Paired
645 quantification cycle (Cq) analysis for the RNase P amplification values obtained by RT-qPCR for
646 each sample assessed. (B) Cq mean \pm standard deviation (mean \pm SD) for the RNase P
647 amplification obtained by RT-qPCR for all the samples evaluated. (C) Paired relative fluorescence
648 unit (RFU) analysis for the RNase P amplification values obtained by RT-qPCR for each sample
649 assessed. (D) RFU mean \pm standard deviation (mean \pm SD) for the RNase P amplification obtained
650 by RT-qPCR from all the samples evaluated. (E) Paired Cq analysis for the SARS-CoV-2 ORF1ab
651 gene amplification values obtained by RT-qPCR for each sample assessed. (F) Paired RFU analysis
652 for the SARS-CoV-2 ORF1ab gene amplification values obtained by RT-qPCR for each sample
653 assessed. (G) RFU mean \pm standard deviation (mean \pm SD) for the SARS-CoV-2 ORF1ab gene
654 amplification obtained by RT-qPCR for all the samples evaluated. (\blacktriangle): positive identification of
655 SARS-CoV-2 positive but no one of the SNV assessed (N501Y, K417N/T, E484K, Hv 69/70 del,
656 P681H). (\blacksquare): positive identification of SARS-CoV-2, and also the SNV N501Y, K417N/T, and
657 E484K. The positive identification of these SNV are suggested for the presence of the P1 SARS-

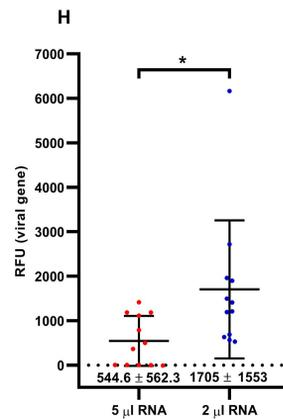
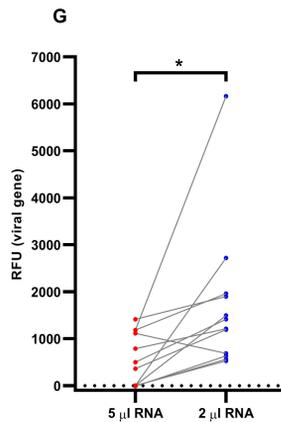
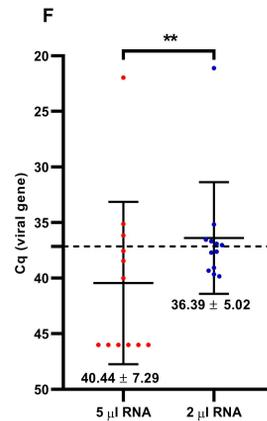
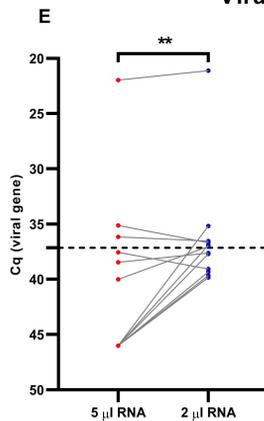
658 CoV-2 variant in the sample. For statistical analysis, paired two-sided Student T-test was applied
659 (n= 90 NPS samples chosen at random). * $p<0.05$; ** $p<0.01$; *** $p<0.001$; **** $p<0.0001$.

660

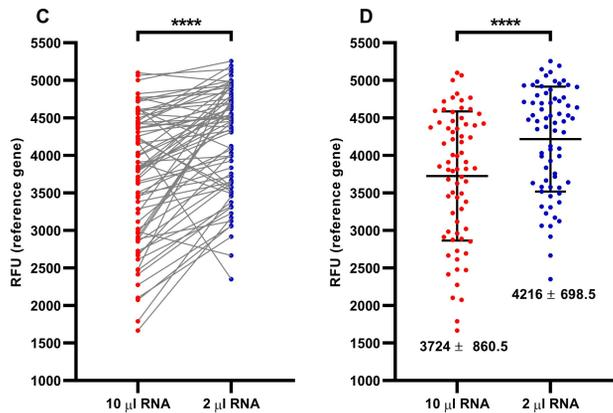
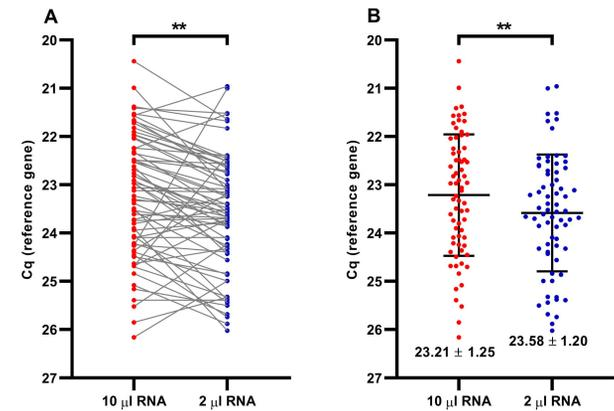
Reference gene



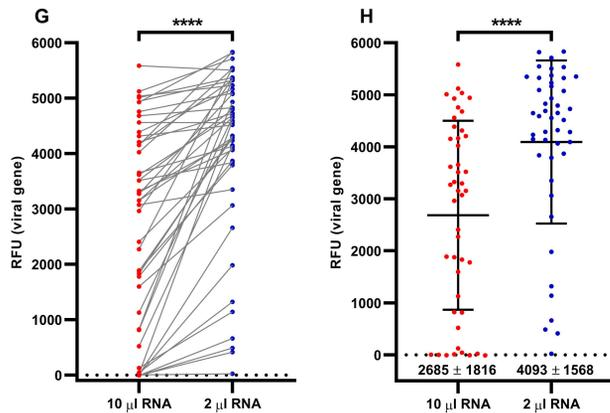
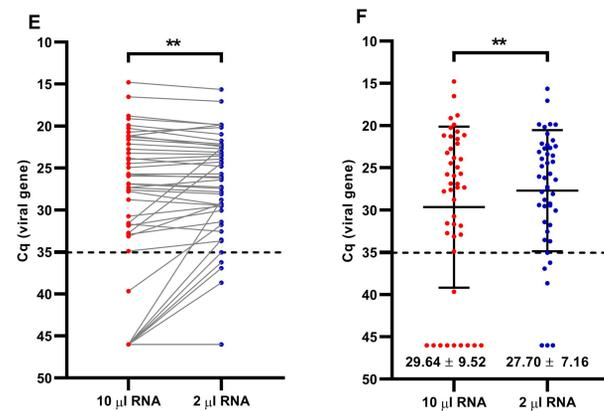
Viral gene



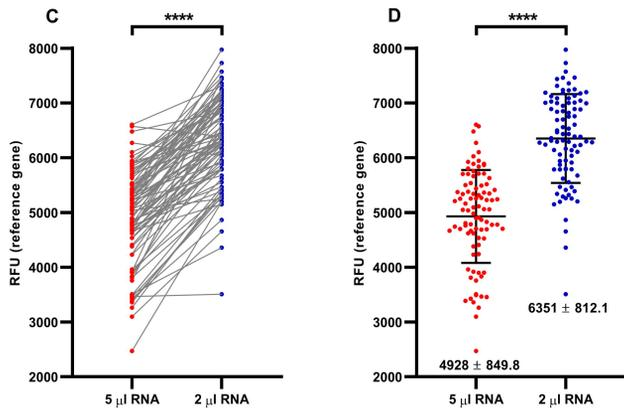
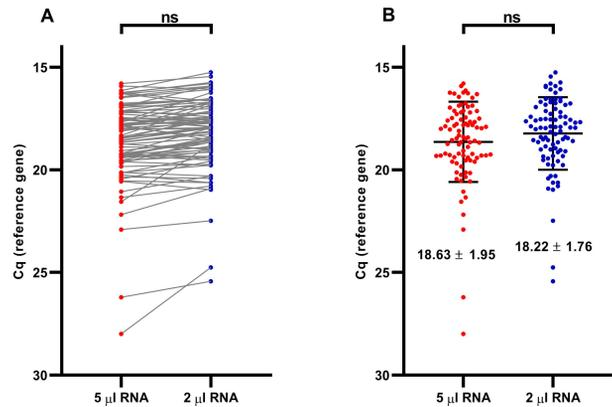
Reference gene



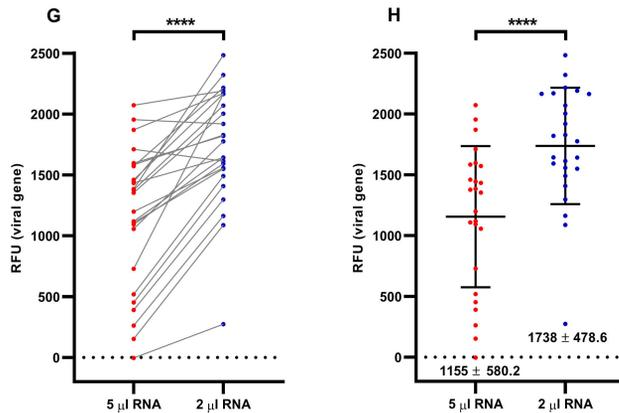
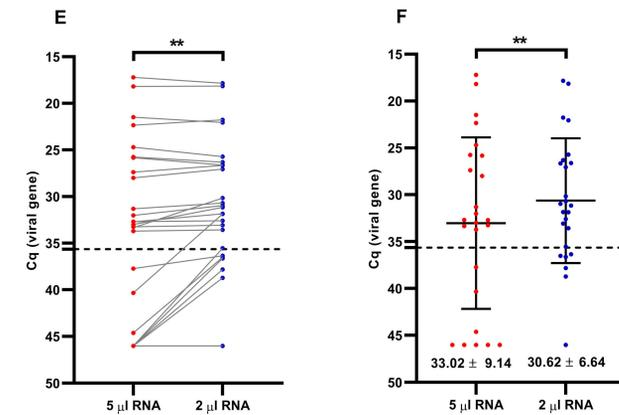
Viral gene



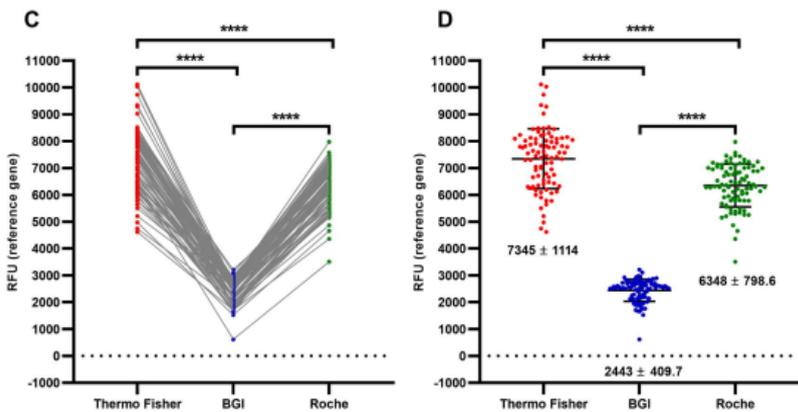
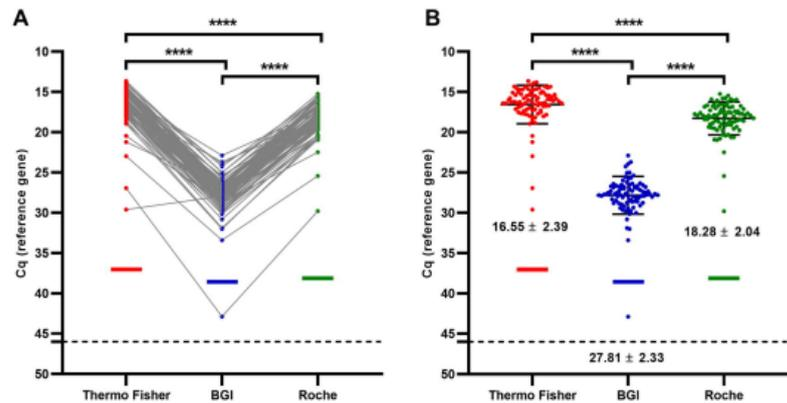
Reference gene



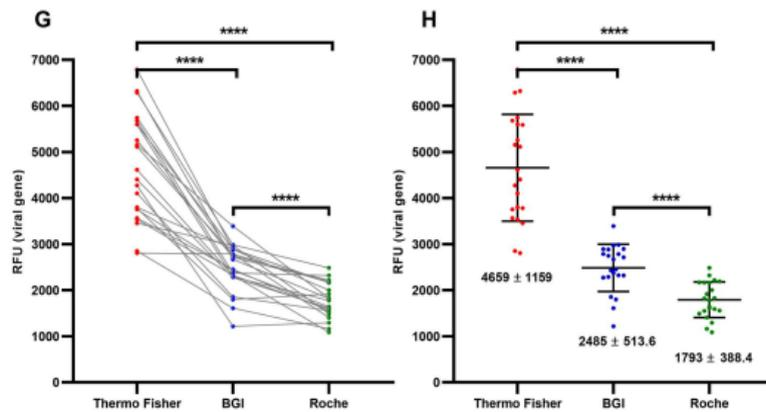
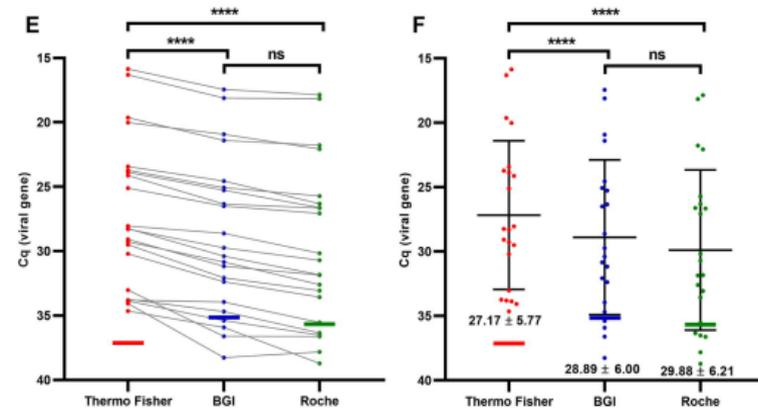
Viral gene



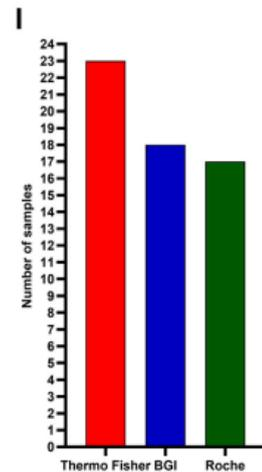
Reference gene



Viral gene



Positive samples

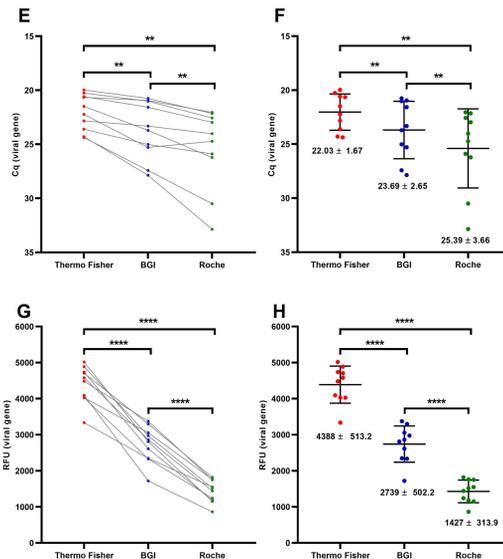
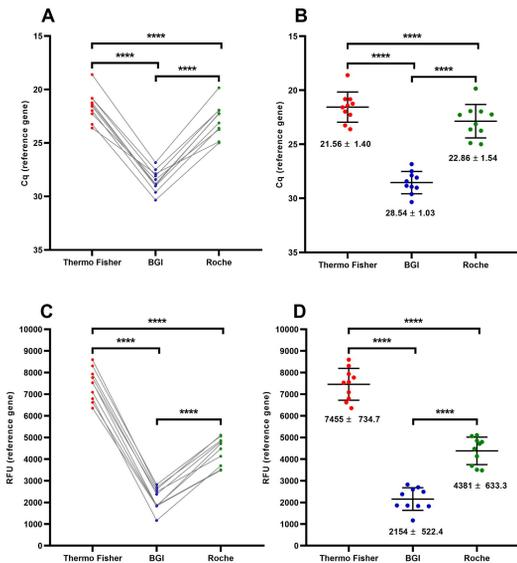


Reference gene

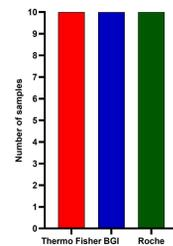
Viral gene

Positive samples

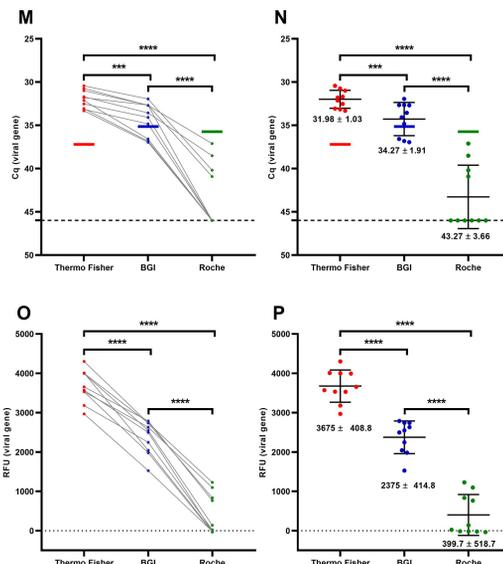
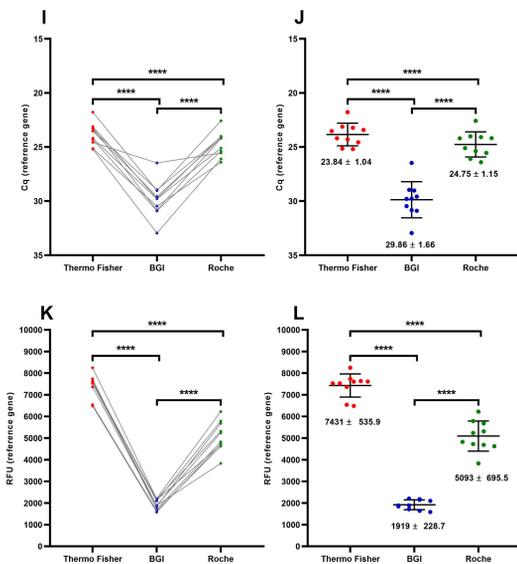
Low Cq values



Q



High Cq values



R

